Inorg. Chem. **2003**, *42*, 3416–3422

Recognition of Topological Isomerism: Synthesis, Structure, and Magnetic Properties of Two Pentanuclear High-Spin Molecules of the Type $[Ni^{II}(N\text{-}N)_2]_3[Fe^{III}(CN)_6]_2$

Curtis P. Berlinguette, José Ramón Galán-Mascarós,† and Kim R. Dunbar*

Department of Chemistry, Texas A&M University, College Station, Texas 77842-3012

Received August 7, 2002

The syntheses, structures, and magnetic properties of two pentanuclear cyanide-bridged compounds are reported. The trigonal bipyramidal molecule $\{[Ni(tmphen)_2]_3[Fe(CN)_6]_2\}\cdot 14H_2O$, (**1**)·$14H_2O$ (tmphen = 3,4,7,8-tetramethyl-1,10-phenanthroline) crystallizes in the space group $P2_1/c$ (No. 14) with unit cell parameters $a = 19.531(4)$ Å, $b = 24.895(5)$ Å, $c = 24.522(5)$ Å, $\beta = 98.68(3)°$, $V = 11787(4)$ Å^3, and $Z = 4$. The π–π interactions between the tmphen ligands provide the closest intermolecular contacts of 3.37 Å leading to large intermolecular M···M distances (> 8.68 Å). The dc magnetic susceptibility of **1** indicates a ferromagnetically coupled $S = 4$ ground state best fit to the parameters $g = 2.23$, $J = +4.3$ cm^{-1}, and $D_{Ni} = +8.8$ cm^{-1} for the Hamiltonian $\hat{H} = -2J[(\hat{S}_{Fe(1)} + \hat{S}_{Fe(2)})\cdot(\hat{S}_{Ni(1)} + \hat{S}_{Ni(2)} + \hat{S}_{Ni(3)})] + D[\hat{S}_{Ni(1)z}^2 + \hat{S}_{Ni(2)z}^2 + \hat{S}_{Ni(3)z}^2]$. The extended square molecule $[Ni(bpy)_2(H_2O)]\{[Ni(bpy)_2]_2[Fe(CN)_6]_2\}\cdot 12H_2O$, (**2**)·$12H_2O$ (bpy = 2,2′-bipyridine) crystallizes in the space group $P\bar{1}$ (No. 2) with unit cell parameters $a = 13.264(3)$ Å, $b = 17.607(4)$ Å, $c = 18.057(4)$ Å, $\alpha = 94.58(3)°$, $\beta = 103.29(3)°$, $\gamma = 95.18(3)°$, $V = 4065(2)$ Å^3, and $Z = 2$. The π–π interactions of 3.29 Å between the bpy ligands are the closest intermolecular contacts, and the intermolecular M···M separations are greater than 7.76 Å. The dc magnetic susceptibility data for **2** are also in accord with an $S = 4$ ground state arising from intramolecular ferromagnetic coupling. The data were best fit to the parameters $g = 2.25$, $J = J' = +3.3$ cm^{-1}, and $D_{Ni} = +5.8$ cm^{-1} for the Hamiltonian $\hat{H} = -2J[(\hat{S}_{Fe(1)} + \hat{S}_{Fe(2)})\cdot(\hat{S}_{Ni(1)} + \hat{S}_{Ni(2)})] - 2J'[(\hat{S}_{Fe(2)}\cdot\hat{S}_{Ni(3)})] + D[\hat{S}_{Ni(1)z}^2 + \hat{S}_{Ni(2)z}^2 + \hat{S}_{Ni(3)z}^2]$. No evidence for long-range magnetic ordering was observed for crystalline samples of **1** or **2**.

Introduction

The field of research based on molecule-based magnets has experienced remarkable growth in the past decade.[1] It is now well-recognized that coordination compounds are ideal building blocks for a variety of solid state materials including room temperature[2] and high coercivity[3] magnets. One of the most fertile areas in molecular magnetism is transition metal cyanide chemistry,[4] a consequence of the fact that the cyanide bridge promotes relatively strong and predictable magnetic coupling between paramagnetic metal centers. In addition to new magnetic materials inspired by 3-D "Prussian-blue" phases, lower dimensional cyanide arrays[5,6] have been synthesized from metal complexes whose ligand environment precludes the formation of an extended face-centered cubic structure.

The chemistry of metal cyanides entered a new phase in recent years due to the considerable interest in large spin paramagnetic molecules[7] that behave as "single-molecule magnets", a term that reflects the fact that the molecule itself is capable of being thermally blocked in a magnetized state.[8] The majority of documented cases of SMM behavior involve

* Author to whom correspondence should be addressed. Phone: (979) 845-5235. Fax: (979) 845-7177. E-mail: dunbar@chem.mail.tamu.edu.

† Present address: Instituto de Ciencia Molecular de la Universidad de Valencia, Spain.

(1) Miller, J. S., Epstein, A. J., Eds. *MRS Bull.* **2000**, *25*, 21−71.

(2) (a) Entley, W. R.; Girolami, G. S. *Inorg. Chem.* **1994**, *33*, 5165−5166. (b) Ferlay, S.; Mallah, T.; Ouahés, R.; Veillet, P.; Verdaguer, M. *Nature* **1995**, *378*, 701−703.

(3) (a) Kurmoo, M.; Kepert, C. J. *New J. Chem.* **1998**, *22*, 1515−1524. (b) Manson, J. L.; Kmety, C. R.; Huang, Q. Z.; Lynn, J. W.; Bendele, G. M.; Pagola, S.; Stephens, P. W.; Liable-Sands, L. M.; Rheingold, A. L.; Epstein, A. J.; Miller, J. S. *Chem. Mater.* **1998**, *10*, 2552−2560. (c) Batten, S. R.; Jensen, P.; Moubaraki, B.; Murray, K. S.; Robson, R. *Chem. Commun.* **1998**, 439−440.

(4) Dunbar, K. R.; Heintz, R. A. *Prog. Inorg. Chem.* **1997**, *45*, 283−391.

(5) (a) Ohba, M.; Okawa, H.; Fukita, N.; Hashimoto, Y. *J. Am. Chem. Soc.* **1997**, *119*, 1011−1019. (b) Smith, J. A.; Galán-Mascarós, J. R.; Clérac, R.; Dunbar, K. R. *Chem. Commun.* **2000**, 1077−1078.

(6) (a) Ohba, M.; Usuki, N.; Fukita, N.; Okawa, H. *Inorg. Chem.* **1998**, *37*, 3349−3354. (b) Kou, H. Z.; Si, S. F.; Gao, S.; Liao, D. Z.; Jiang, Z. H.; Yan, S. P.; Fan, Y. G.; Wang, G. L. *Eur. J. Inorg. Chem.* **2002**, 699−702.

10.1021/ic0205031 CCC: $25.00
Published on Web 05/03/2003

Scheme 1. Convergent Precursors: Metals Coordinated with Two Bidentate Ligands, Which Leaves Two Cis Sites Available for Coordination

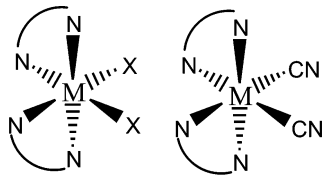

N-N = bidentate ligand
X = leaving group (e.g. halide)

discrete fragments of manganese oxides, but efforts to use cyanide ligands to prepare high-spin clusters are underway in a number of laboratories. For example, researchers are using convergent precursors to favor the deliberate formation of molecular squares and cubes with bridging cyanide ligands (Scheme 1).[9,10] A logical extension of the all-convergent building-block approach is to combine a divergent precursor such as a cyanometalate anion with a convergent metal cation complex, chemistry that is subject to multiple product formation due to competition between energetically similar structures (e.g., closed and open frameworks).[11,12]

The synthetic obstacles in molecular magnetism to prepare bulk crystalline phases are particularly prevalent in cyanide chemistry, which can result in problems when one attempts to relate the structure of a single crystal to the magnetism of a bulk sample. Herein we report the results of a detailed investigation of the structure/property relationships of two clusters obtained from reactions between $[Fe(CN)_6]^{3-}$ and $Ni(N\text{-}N)_2X_2$ (N-N = bpy, tmphen; X = counteranion), one of which exhibits an unprecedented "extended square" molecular geometry. Magnetic data obtained on batches of single crystals indicate that both isomers exhibit intramolecular ferromagnetic coupling between the Ni^{II} and Fe^{III} spin centers to stabilize a high-spin ground state of $S = 4$. In contrast to previous reports of related Ni_3Fe_2 clusters,[13] we found no evidence of long-range magnetic ordering between trigonal bipyramidal clusters of type $\{[Ni^{II}(N\text{-}N)_2]_3[Fe^{III}(CN)_6]_2\}$ mediated by hydrogen bonding.

Experimental Section

Starting Materials. The starting materials $NiCl_2 \cdot 6H_2O$ and $K_3[Fe(CN)_6]$ were purchased from Fisher Scientific and used without further purification. The reagents 2,2′-bipyridine (bpy), 3,4,7,8-tetramethyl-1,10-phenanthroline (tmphen), and 18-crown-6 were purchased from Aldrich and used without further purification. The salt $[(18\text{-crown-}6)K]_3[Fe(CN)_6]$ was prepared in situ by stirring an excess of $K_3[Fe(CN)_6]$ in a solution of 18-crown-6 in methanol.

Physical Measurements. Infrared (IR) spectra were measured as Nujol mulls between KBr plates on a Nicolet 740 FT-IR spectrometer. Magnetic susceptibility and magnetization measurements were carried out with a Quantum Design SQUID magnetometer MPMS-XL. DC magnetic measurements were performed with an applied field of 1000 G in the 2−300 K temperature range. Ac magnetic susceptibility measurements were performed in a 3 G ac field at an operating frequency of 997 Hz. Magnetization data was collected in the 0−7 T range starting at zero field at 2 K. Data were corrected for the diamagnetic contributions calculated from the Pascal constants.[14]

Syntheses. $\{[Ni(tmphen)_2]_3[Fe(CN)_6]_2\}\cdot 14H_2O$, (1)·$14H_2O$. A sample of $NiCl_2 \cdot 6H_2O$ (40 mg, 0.17 mmol) was dissolved in 30 mL of methanol and combined with 2 equiv of tmphen (80 mg, 0.34 mmol) dissolved in 20 mL of methanol. This solution was then combined with a 50 mL methanol solution of $[(18\text{-crown-}6)K]_3[Fe(CN)_6]$ (220 mg, 0.20 mmol), and the reaction mixture was left to stand undisturbed for 1 week. Orange crystals were obtained: yield = 0.35 mg (∼30%). IR (Nujol): 2151, 2141, 2111, 2064 cm^{-1}; ν(C≡N). TGA measurements on dried crystals support 11 H_2O molecules per molecular unit.[15]

$[Ni(bpy)_2(OH_2)]\{[Ni(bpy)_2]_2[Fe(CN)_6]_2\}\cdot 12H_2O$, (2)·$12H_2O$. A quantity of $NiCl_2 \cdot 6H_2O$ (20.0 mg, 0.08 mmol) was dissolved in 15 mL of methanol and combined with 2 equiv of bpy (25 mg, 0.16 mmol) in 20 mL of methanol. This solution was then layered over a solution of $K_3[Fe(CN)_6]$ (100 mg, 0.30 mmol) dissolved in 20 mL of water. During the period of 2−3 weeks, dark orange blocks grew near the interface of the layers: Yield = 5 mg (∼1%). IR (Nujol): 2147, 2119, 2110, 2067 cm^{-1}; ν(C≡N). TGA measurements on dried crystals support the presence of 9 H_2O molecules per molecular unit in a typical dried sample.[15]

Single-Crystal X-ray Diffraction Studies. X-ray data sets were collected on a SMART 1K area detector diffractometer equipped with graphite-monochromated Mo Kα radiation ($\lambda_\alpha = 0.71073$ Å). The frames were integrated in the Siemens SAINT[16] software package, and the data was corrected for absorption using the SADABS program.[17] The structures were solved using the direct-methods program SIR97[18] and refined in the SHELXL-97 package.[19]

An orange crystal of $\{[Ni(tmphen)_2]_3[Fe(CN)_6]_2\}\cdot 14H_2O$, (**1**)·$14H_2O$ ($0.17 \times 0.16 \times 0.11$ mm^3) was secured on the tip of a

(7) (a) Zhong, Z. J.; Seino, H.; Mizobe, Y.; Hidai, M.; Fujishima, A.; Ohkoshi, S.; Hashimoto, K. *J. Am. Chem. Soc.* **2000**, *122*, 2952−2953. (b) Larionova, J.; Mathias, G.; Pilkington, M.; Andres, H.; Stoeckli-Evans, H.; Güdel, H. U.; Decurtins, S. *Angew. Chem., Int. Ed.* **2000**, *39*, 1605−1609. (c) Sculiller, A.; Mallah, T.; Verdaguer, M.; Nivorozkhin, A.; Tholence, J. L.; Veillet, P. *New J. Chem.* **1996**, *20*, 1−3.

(8) (a) Sessoli, R.; Tsai, H.-L.; Schake, A. R.; Wang, S.; Vincent, J. B.; Folting, K.; Gatteschi, D.; Christou, G.; Hendrickson, D. N. *J. Am. Chem. Soc.* **1993**, *115*, 1804−1816. (b) Christou, G.; Gatteschi, D.; Hendrickson, D. N.; Sessoli, R. *MRS Bull.* **2000**, *25*, 66. (c) Wernsdorfer, W.; Aliaga-Alcalde, N.; Hendrickson, D. N.; Christou, G. *Nature* **2002**, *416*, 406−409.

(9) (a) Oshio, H.; Tamada, O.; Onodera, H.; Ito, T.; Ikoma, T.; Tero-Kubota, S. *Inorg. Chem.* **1999**, *38*, 5686−5689. (b) Klausmeyer, K. K.; Rauchfuss, T. B.; Wilson, S. R. *Angew. Chem., Int. Ed.* **1998**, *37*, 1694−1696.

(10) (a) Berseth, P. A.; Sokol, J. J.; Shores, M. P.; Heinrich, J. L.; Long, J. R. *J. Am. Chem. Soc.* **2000**, *122*, 9655−9662. (b) Contakes, S. M.; Rauchfuss, T. B. *Angew. Chem., Int. Ed.* **2000**, *39*, 1984−1986.

(11) (a) Rogez, G.; Parsons, S.; Paulsen, C.; Villar, V.; Mallah, T. *Inorg. Chem.* **2001**, *40*, 3836−3837. (b) Shen, X. P.; Li, B. L.; Zou, J. Z.; Yu, Y. P.; Liu, S. X. *Transition Met. Chem.* **2002**, *27*, 372−376.

(12) (a) Ohba, M.; Okawa, H. *Coord. Chem. Rev.* **2000**, *198*, 313−328. (b) Miyasaka, H.; Ieda, N.; Matsumoto, N.; Re, N.; Creseenzi, R.; Floriani, C. *Inorg. Chem.* **1998**, *37*, 255−263.

(13) (a) Van Langenberg, K.; Batten, S. R.; Berry, K. J.; Hockless, D. C. R.; Moubaraki, B.; Murray, K. S. *Inorg. Chem.* **1997**, *36*, 5006−5015. (b) Langenberg, K. V.; Hockless, D. C. R.; Moubaraki, B.; Murray, K. S. *Synth. Met.* **2001**, *122*, 573−580.

(14) *Theory and Applications of Molecular Paramagnetism*; Boudreaux, E. A., Mulay, L. N., Eds; John Wiley & Sons: New York, 1976.

(15) TGA data for compounds **1** and **2** are submitted as Supporting Information as Figures S1 and S2, respectively.

(16) *SAINT, Program for area detector absorption correction*; Siemens Analytical X-Ray Instruments Inc.: Madison, WI, 1994−1996.

(17) Program in the SHELXL-97 software.

(18) Altomare, A.; Burla, M. C.; Camalli, M.; Cascarano, G. L.; Giacovazza, C.; Guagliardi, A.; Moliterni, A. G. G.; Polidori, G.; Spagna, R. *J. Appl. Crystallogr.* **1999**, *32*, 115.

(19) Sheldrick, G. M. *SHELXL-97, Program for refining crystal structures*; University of Göttingen: Göttingen, 1997.

Table 1. Crystallographic Data and Structural Refinement Parameters for $\{[Ni(tmphen)_2]_3[Fe(CN)_6]_2\}\cdot 14H_2O$, (**1**)·$14H_2O$, and $[Ni(bpy)_2(OH_2)]\{[Ni(bpy)_2]_2[Fe(CN)_6]_2\}\cdot 12H_2O$, (**2**)·$12H_2O$

	1·$14H_2O$	**2**·$12H_2O$
chemical formula	$C_{108}H_{124}Fe_2N_{24}Ni_3O_{14}$	$C_{72}H_{74}Fe_2N_{24}Ni_3O_{13}$
a (Å)	19.531(4)	13.264(3)
b (Å)	24.895(5)	17.607(4)
c (Å)	24.522(5)	18.057(4)
α (deg)	90	94.58(3)
β (deg)	98.68(3)	103.29(3)
γ (deg)	90	95.18(3)
V (Å^3)	11787(4)	4065(2)
Z	4	2
fw	2270.14	1771.28
space group	$P2_1/c$ (No. 14)	$P\bar{1}$ (No. 2)
T (K)	110(2)	110(2)
λ (Å)	0.71073	0.71069
D_{calc} (g cm^{-3})	1.279	1.434
μ (cm^{-1})	7.78	11.03
$R(F_o)^a$	0.0774	0.0720
$R_w(F_o^2)^b$	0.1652[c]	0.1538[d]

[a] $R(F_o) = \sum[(F_o - F_o)]/\sum(F_o)$. [b] $R_w(F_o^2) = \{\sum[w(F_o^2 - F_c^2)^2]/\sum[w(F_o^2)^2]\}^{1/2}$. [c] $w = 1/[\sigma^2(F_o^2) + (0.0904P)^2]$ where $P = (F_o^2 + 2F_c^2)/3$. [d] $w = 1/[\sigma^2(F_o^2) + (0.0909P)^2]$ where $P = (F_o^2 + 2F_c^2)/3$.

glass fiber with Dow Corning silicone grease and placed in a cold N_2(g) stream at 110(2) K. A total of 28608 unique reflections were collected, although it should be pointed out that the data set was weak due to the small size of the crystal. The crystal system was determined to be monoclinic, $P2_1/c$. All non-hydrogen atoms were located after successive Fourier difference maps, but due to the low data to parameter ratio, only the metal atoms were refined anisotropically. Hydrogen atoms were placed in calculated positions, and their thermal parameters were fixed to be 20% larger than those of the atoms to which they are bound (50% in the case of methyl groups). The water molecules in the interstices of the crystal are highly disordered. The best fitting was obtained by assigning the electron density to water molecules with occupancy factors less than 1 (from 1.00 down to 0.15). The final refinement cycle was based on 5476 reflections with $F_o > 4\sigma(F_o)$ and 783 parameters (R1 = 0.0774 and wR2 = 0.1652).

A dark orange crystal of $[Ni(bpy)_2(OH_2)]\{[Ni(bpy)_2]_2[Fe(CN)_6]_2\}\cdot 12H_2O$, (**2**)·$12H_2O$ (0.10 × 0.08 × 0.08 mm^3), was secured on the tip of a glass fiber with Dow Corning silicone grease and placed in a cold N_2(g) stream at 110(2) K. A total of 18620 unique reflections were collected, and the space group was determined to be triclinic $P\bar{1}$. All non-hydrogen atoms were located, but only the metal atoms were refined anisotropically. Hydrogen atoms were placed in calculated positions, with the exception of the two H atoms associated with the water molecule bound to the Ni3 atom, which were located and refined; the O−H distances were constrained to be the same value. The thermal parameters of all hydrogen atoms were fixed to be 20% larger than those of the atoms to which they are bonded. As in the case of **1**, disordered water molecules in the interstices were modeled with various occupancy factors less than 1 (from 0.90 to 0.10). The final refinement cycle was based on 4093 reflections with $F_o > 4\sigma(F_o)$ and 558 parameters (R1 = 0.0720 and wR2 = 0.1538).

Crystal parameters and basic information pertaining to data collection and refinement for both structures are summarized in Table 1. Important bonding distances and angles are listed in Tables 2 and 3.

Results

Syntheses and Molecular Structures. $\{[Ni(tmphen)_2]_3[Fe(CN)_6]_2\}\cdot 14H_2O$ (1). The successful isolation of pure samples of **1** and **2** from these reactions depends on several factors, in particular the choice of solvent and capping ligand. Although the yields of the pure phases as single crystals are low, purity is crucial if one is attempting to correlate the physical properties with the structure of a compound.[20,21] The preparation of **1** does not require strict anhydrous conditions, but the reaction cannot be carried out in aqueous media. This

Table 2. Selected Bond Distances (Å) and Angles (deg) for (**1**)·$14H_2O$

Ni(1)−Ni(1)	2.081(7)	Fe(1)−C(123)	1.906(11)
Ni(1)−N(2)	2.069(7)	Fe(1)−C(121)	1.887(11)
Ni(1)−N(3)	2.104(7)	Fe(1)−C(126)	1.926(9)
Ni(1)−N(4)	2.096(7)	Fe(1)−C(124)	1.930(9)
Ni(1)−N(126)	2.070(7)	Fe(1)−C(122)	1.922(10)
Ni(1)−N(136)	2.004(7)	Fe(1)−C(125)	1.935(10)
N(126)−C(126)	1.180(9)		
C(121)−Fe(1)−C(122)	93.1(4)	N(1)−Ni(1)−N(2)	78.7(3)
C(121)−Fe(1)−C(123)	89.0(4)	Ni(1)−Ni(1)−N(3)	86.8(3)
C(121)−Fe(1)−C(124)	86.1(4)	N(1)−Ni(1)−N(4)	90.9(3)
C(121)−Fe(1)−C(125)	89.4(4)	N(1)−Ni(1)−N(126)	91.0(3)
C(121)−Fe(1)−C(126)	176.5(4)	N(1)−Ni(1)−N(136)	173.5(3)
Fe(1)−C(126)−N(126)	172.4(8)	Ni(1)−N(126)−C(126)	157.9(7)

Table 3. Selected Bond Distances (Å) and Angles (deg) for (**2**)·$12H_2O$

Ni(1)−N(7)	2.052(9)	Fe(2)−C(11)	1.917(10)
Ni(1)−N(1)	2.055(9)	Fe(2)−C(9)	1.923(11)
Ni(1)−N(22)	2.069(8)	Fe(2)−C(10)	1.925(12)
Ni(1)−N(32)	2.097(9)	Fe(2)−C(7)	1.940(11)
Ni(1)−N(31)	2.105(9)	Fe(2)−C(12)	1.945(12)
Ni(1)−N(21)	2.129(9)	Fe(2)−C(8)	1.962(11)
Ni(2)−N(8)	2.046(9)	N(1)−C(1)	1.155(11)
Ni(2)−N(2)	2.069(9)	N(2)−C(2)	1.152(11)
Ni(3)−N(9)	2.050(9)	N(7)−C(7)	1.155(12)
Ni(3)−O(1)	2.077(11)	Ni(8)−C(8)	1.148(11)
Fe(1)−C(2)	1.939(11)	N(9)−C(9)	1.158(12)
Fe(1)−C(1)	1.941(11)		
N(7)−Ni(1)−N(1)	91.5(3)	Fe(1)−C(1)−N(1)	176.4(10)
N(7)−Ni(1)−N(21)	172.0(3)	Fe(1)−C(2)−N(2)	177.9(10)
N(7)−Ni(1)−N(22)	93.2(3)	C(2)−Fe(1)−C(1)	88.4(4)
N(7)−Ni(1)−N(31)	91.0(3)	C(7)−Fe(2)−C(8)	91.2(4)
N(7)−Ni(1)−N(32)	95.6(3)	C(7)−Fe(2)−C(9)	177.8(5)
Ni(1)−N(1)−C(1)	167.5(9)	C(7)−Fe(2)−C(10)	93.2(5)
Ni(1)−N(7)−C(7)	170.3(9)	C(7)−Fe(2)−C(11)	90.1(4)
Ni(2)−N(2)−C(2)	159.2(9)	C(7)−Fe(2)−C(12)	90.7(5)
Ni(2)−N(8)−C(8)	172.4(9)	C(11)−Fe(2)−C(9)	88.1(4)
N(8)−Ni(2)−N(2)	90.3(3)	Fe(2)−C(8)−N(8)	173.2(9)
Ni(3)−N(9)−C(9)	151.8(9)	Fe(2)−C(9)−N(9)	172.5(10)
O(1)−Ni(3)−N(9)	85.5(4)	Fe(2)−C(7)−N(7)	175.1(10)

(20) If the diffusion of reagents is not carried out slowly, the combination of $[(18\text{-crown-}6)K]_3[Fe(CN)_6]$ and $Ni(tmphen)_2Cl_2$ results in the formation of a brown insoluble microcrystalline solid (IR (Nujol): 2157, 2145, 2116, 2105 cm^{-1}; ν(C≡N)). Structural characterization of this solid product by powder XRD techniques proved to be unsuccessful. The thermal variation product, $\chi_m T$, of the solid is indicative of ferromagnetic coupling analogous to that in compound **1**. The solid exhibits long-range magnetic ordering evidenced by ac susceptibility measurements (T_c = 14 K) and hysteretic behavior (H_c = 180 G at T = 2 K). The magnetic properties of this solid are in the Supporting Information (Figures S5−S7).

(21) The bulk reaction of $K_3[Fe(CN)_6]$ and $Ni(bpy)_2Cl_2$ leads to the formation of a brown insoluble microcrystalline solid (IR: 2159, 2145, 2113, 2106 cm^{-1}; ν(C≡N)). The thermal variation of $\chi_m T$ is indicative of ferromagnetic coupling similar to that in compound **2**. The solid exhibits long-range magnetic ordering evidenced by ac susceptibility measurements (T_c = 11 K) and hysteretic behavior (H_c = 690 G at T = 2 K) which can be found in the Supporting Information (Figures S8−S10). The contamination of this solid in samples of **2** led to a preliminary report that the cluster exhibited magnetic ordering (Smith, J. A.; Galán-Mascarós, J. R.; Clerac, R.; Sun, J.-S.; Ouyang, X.; Dunbar, K. R. *Polyhedron* **2001**, *20*, 1727−1734). Subsequently, a larger quantity of **2** was prepared, and the magnetic data do not show evidence for long-range magnetic ordering.

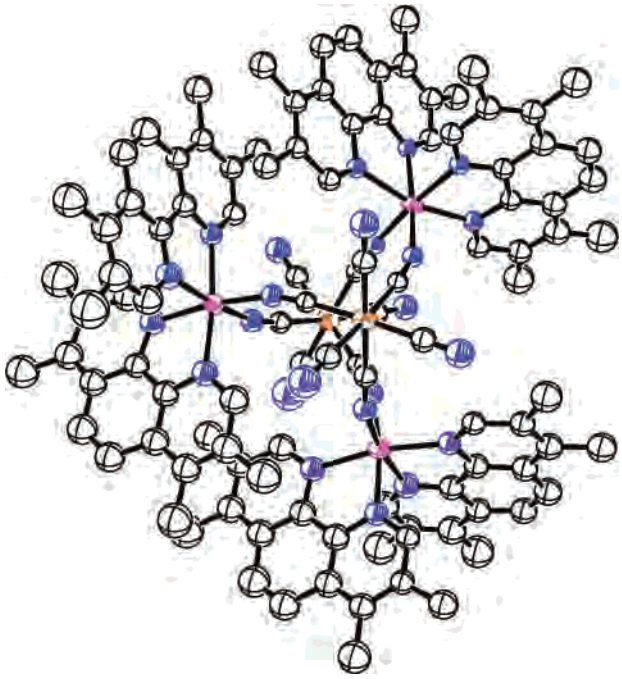

Figure 1. ORTEP representation of $\{[Ni(tmphen)_2]_3[Fe(CN)_6]_2\}$ (**1**), drawn at the 50% probability level (Fe = orange; Ni = pink; H atoms omitted for clarity).

being the case, it is necessary to use polypyridyl ligands that promote better solubility of the starting material and products in organic solvents. The best results were obtained with 3,4,7,8-tetramethyl-1,10-phenanthroline (tmphen) in methanol. The product isolated from these reaction conditions is $\{[Ni(tmphen)_2]_3[Fe(CN)_6]_2\}\cdot 14H_2O$, (**1**)$\cdot 14H_2O$, which is analogous to other trigonal bipyramidal compounds of general formula $\{[Ni(L\text{-}L)_2]_3[Fe(CN)_6]_2\}$ (L-L = bis(1-pyrazolyl)methane, 2,2′-bipyridine, 2-pyridyl-iminonitroxide).[13,22] In this compound, $\{Ni(tmphen)_2\}^{2+}$ units are situated in the equatorial plane and are connected to the apical $[Fe(CN)_6]^{3-}$ units via the N end of three fac CN^- ligands (Figures 1 and 2). All three $\{Ni(tmphen)_2\}^{2+}$ moieties within one cluster exhibit identical chiralities (all Λ or all Δ), but both homochiral enantiomers are present in the crystal, which leads to a centrosymmetric space group ($P2_1/c$). The $\pi-\pi$ contacts (3.37 Å) between the tmphen ligands provide the shortest *intermolecular* interactions (Figure 3). The clusters can be considered to be magnetically well isolated from each other as evidenced by the fact that all *intermolecular* metal···metal distances are greater than 8 Å (Ni···Ni = 8.68 Å; Fe···Ni 9.19 Å). The terminal cyanide ligands maintain close contacts to several disordered solvent water molecules (O···N distances ≥ 2.82 Å and up), but do not form a well-defined hydrogen-bonding network between the clusters.

$[Ni(bpy)_2(OH_2)]\{[Ni(bpy)_2]_2[Fe(CN)_6]_2\}\cdot 12H_2O$ (2). In order to obtain crystals of **2**, it is necessary to very slowly mix an aqueous solution of $K_3[Fe(CN)_6]$ with a methanol or acetonitrile solution of the in situ prepared precursor, $\{Ni(bpy)_2\}^{2+}$. The molecular structure of **2** consists of neutral molecules of the type $[Ni(bpy)_2(OH_2)]\{[Ni(bpy)_2]_2[Fe(CN)_6]_2\}$

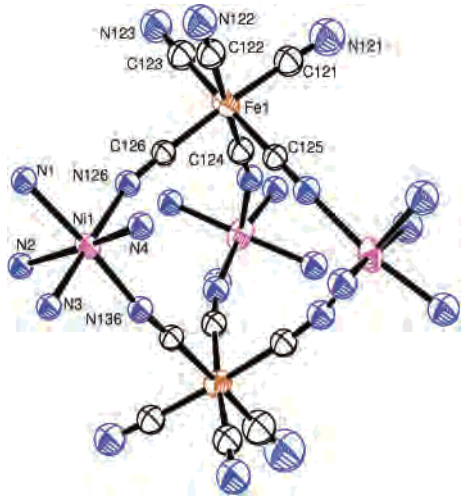

Figure 2. ORTEP plot of the trigonal bipyramidal core of compound **1**. For clarity, only the N atoms of the tmphen ligand are included. (Fe = orange; Ni = pink).

(Figure 4) whose basic geometry is that of an "extended square". The basic square motif is $\{[Ni(bpy)_2]_2[Fe(CN)_6]_2\}^{2-}$ with the four metal ions serving as corners and four bridging CN^- ligands acting as edges. Two cis positions of the $\{Ni(bpy)_2\}^{2+}$ precursor are coordinated to cis CN^- ligands from independent $[Fe(CN)_6]^{3-}$ units to yield a cyclic unit. Each square contains one Δ and one Λ Ni complex. In addition, one of the $[Fe(CN)_6]^{3-}$ corners is bound to a third $\{Ni(bpy)_2\}^{2+}$ unit through one of the CN^- units that lies in the plane of the square. This $\{Ni(bpy)_2\}^{2+}$ "appendage" is coordinated to a water molecule that is hydrogen-bonded to the CN^- ligand of the $[Fe(CN)_6]^{3-}$ corner unit (O···N distance = 3.15 Å). This interaction leads to a deviation from linearity for the $Fe_{square}-C\equiv N-Ni_{appendage}$ bridge ($\angle C-N-Ni_{appendage} = 151.6(9)°$). This bent angle is not unprecedented, as angles as acute as C−N−Ni = 122° and C−N−Cu = 120° have been documented.[23,24] As was observed for crystals of **1**, disordered water molecules reside near the terminal cyanide ligands. The $\pi-\pi$ contacts of 3.29 Å between bpy ligands of neighboring clusters provide the closest intermolecular contacts. The intercluster metal distances in **2** are shorter than in **1**, which reflects the different shape of the molecules and the reduced steric bulk of the bpy ligands relative to the substituted tmphen ligands. It is important to note that the *intercluster* metal···metal distances are still quite long, with 7.76 Å being the shortest distance between metal centers. With such distances between spin centers in discrete molecules, the molecules can be considered to be magnetically isolated from each other in the crystals.

Magnetic Properties. Variable-temperature (2−300 K) magnetic susceptibility data were collected on crushed single crystals of $\{[Ni(tmphen)_2]_3[Fe(CN)_6]_2\}\cdot 14H_2O$, (**1**)$\cdot 14H_2O$ (Figure 5). The room temperature $\chi_m T$ value of 4.94 emu K mol^{-1} is in good agreement with the expected value for three

(22) Vostrikova, K. E.; Luneau, D.; Wernsdorfer, W.; Rey, P.; Verdaguer, M. *J. Am. Chem. Soc.* **2000**, *122*, 718−719.

(23) Bellouard, F.; Clemente-León, M.; Coronado, E.; Galán-Mascarós, J. R.; Gómez-García, C. J.; Romero, F.; Dunbar, K. R. *Eur. J. Inorg. Chem.* **2002**, 1603−1606.

(24) Escorihuela, I.; Falvello, L. R.; Tomás, M. *Inorg. Chem.* **2001**, *40*, 636−640.

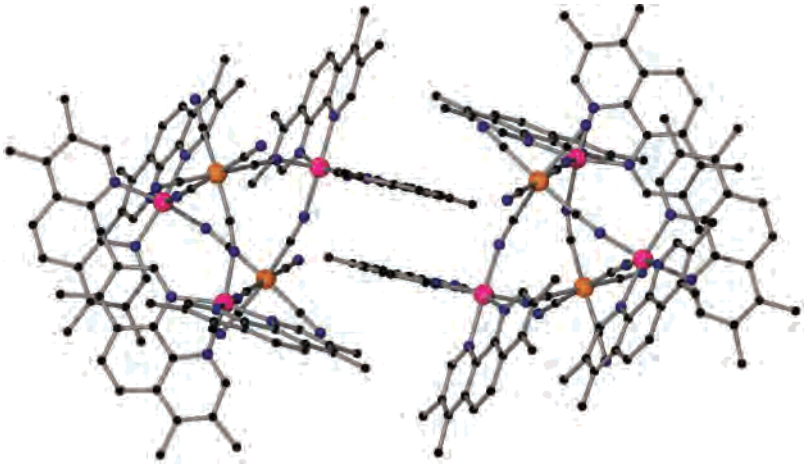

Figure 3. Packing diagram for compound **1** demonstrating the dimerization of the molecules due to $\pi-\pi$ interactions.

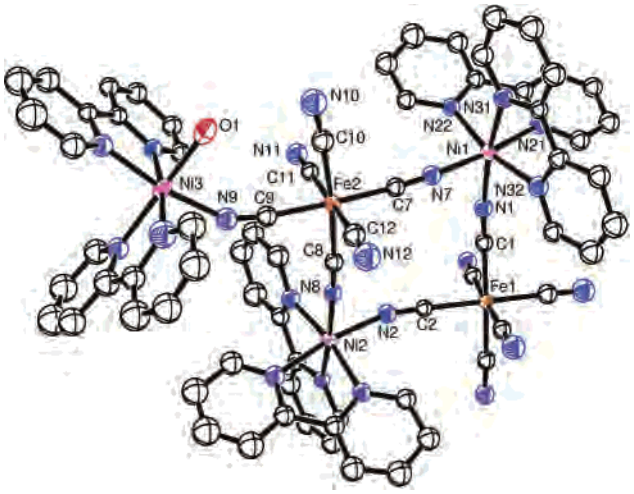

Figure 4. ORTEP representation of $[Ni(bpy)_2(OH_2)]\{[Ni(bpy)_2]_2[Fe(CN)_6]_2\}$ (**2**), drawn at the 50% probability level (Fe = orange; Ni = pink; H atoms omitted for clarity).

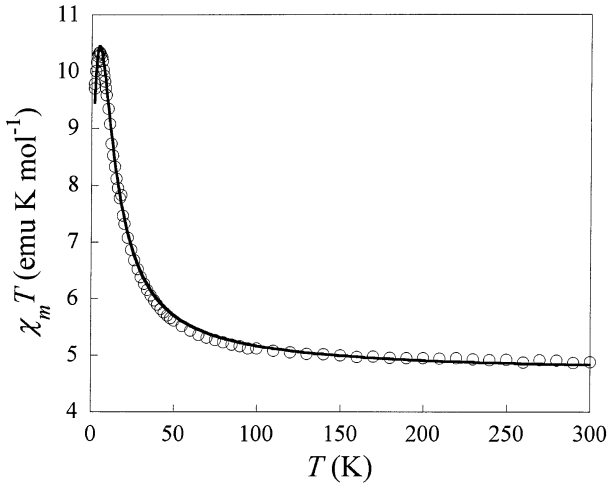

Figure 5. Thermal variation of the $\chi_m T$ product for compound **1** in the 2−300 K range. The solid line shows the best fitting obtained for g = 2.23; J = +4.3 cm^{-1}; D_{Ni} = +8.8 cm^{-1}.

Ni^{II} ions (S = 1) and two low-spin Fe^{III} ions (S = 1/2) that are magnetically isolated (expected value is 3.75 emu K mol^{-1} for g = 2.00). The value of $\chi_m T$ remains relatively temperature independent in the 300−100 K range and then

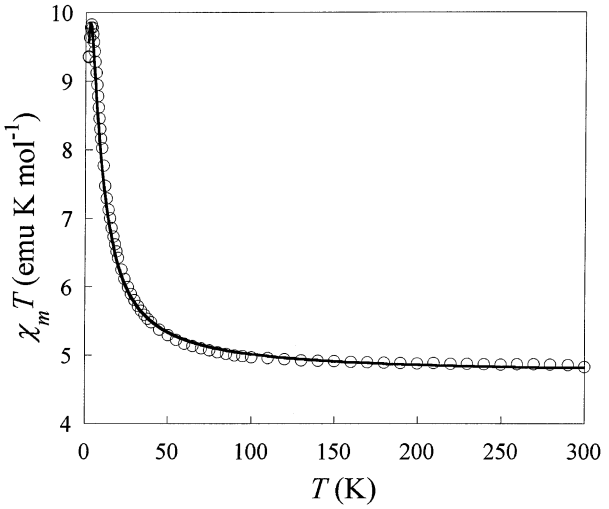

Figure 6. Thermal variation of the $\chi_m T$ product for compound **2** in the 2−300 K range. The solid line shows the best fitting obtained for g = 2.25; $J = J'$ = +3.3 cm^{-1}; D_{Ni} = +5.8 cm^{-1}.

increases rapidly to a maximum of 10.34 emu K mol^{-1} at T = 5.0 K. This behavior is an indication that the superexchange interactions between the metal spin centers are ferromagnetic, as expected for the orthogonal t_{2g} magnetic orbitals of the low-spin Fe^{III} ion and the e_g orbitals of the Ni^{II} ions. The value of $\chi_m T$ decreases at very low temperatures, a feature that is ascribed to zero-field splitting effects, since *intercluster* interactions should be very weak and are probably negligible. As stated in the X-ray crystallographic section, the M···M distances between neighboring clusters are too long to expect significant dipolar interactions and therefore facilitate long-range magnetic ordering. This is supported by the ac susceptibility measurements, which do not reveal evidence of magnetic ordering for pure samples of **1**.[25]

Samples of crushed single crystals of $[Ni(bpy)_2(OH_2)]\{[Ni(bpy)_2]_2[Fe(CN)_6]_2\}\cdot 12H_2O$, (**2**)·$12H_2O$ (Figure 6), exhibit magnetic behavior analogous to that exhibited by compound **1**. The room temperature $\chi_m T$ value of 4.98 emu K mol^{-1} is

(25) Ac susceptibility measurements for compounds **1** and **2** are provided as Supporting Information, Figures S3 and S4, respectively.

Scheme 2. The Exchange Interactions Represented by J and J' for the Trigonal Bipyramidal Geometry for Compound **1** and the Extended Square Geometry for Compound **2**

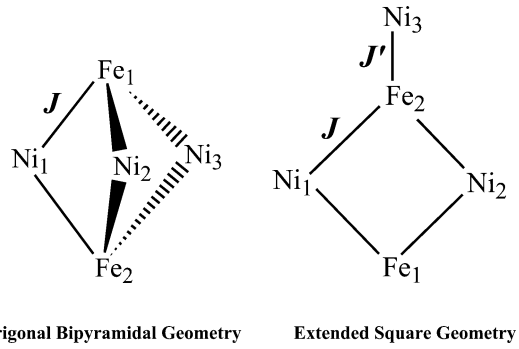

virtually identical to that of **1**, and the maximum value of 9.83 emu K mol^{-1} occurs at $T = 4.2$ K. The similarities in magnetic behavior notwithstanding, the magnetic interactions in the two clusters are not identical. For molecules of type **1**, all six magnetic interactions are related by symmetry and must be of the same sign and magnitude. In the case of **2**, however, the four edges of the square represent a different interaction than the cyanide bridge to the outer Ni atom. Although this is the case, it is noted that all cyanide-bridged Fe···Ni superexchange interactions reported to date are ferromagnetic regardless of the angle subtended by the CN^- bridge.[20] Accordingly, all interactions in compound **2** are expected to be ferromagnetic. Ac susceptibility measurements do not show evidence of long-range magnetic ordering for compound **2**.[25]

Calculations were performed for both compounds by using the magnetism program, MAGPACK.[26] For $\{[Ni(tmphen)_2]_3[Fe(CN)_6]_2\}\cdot 14H_2O$, (**1**)$\cdot 14H_2O$, all the interactions between the Ni^{II} and Fe^{III} spins were treated as isotropic, with identical interactions being defined by the same parameter J (Scheme 2). The Hamiltonian $\hat{H} = -2J[(\hat{S}_{Fe(1)} + \hat{S}_{Fe(2)})\cdot(\hat{S}_{Ni(1)} + \hat{S}_{Ni(2)} + \hat{S}_{Ni(3)})] + D[\hat{S}_{Ni(1)z}^2 + \hat{S}_{Ni(2)z}^2 + \hat{S}_{Ni(3)z}^2]$ represents the exchange interactions and axial zero-field splitting terms for the Ni^{II} ions used in the model. Second neighbor interactions were not taken into account, and a mean g value was used for all the atoms. The best agreement with the data was obtained for $J = +4.3$ cm^{-1}, $g = 2.23$, and $D_{Ni} = +8.8$ cm^{-1} (Figure 5). This set of parameters accurately reproduces all the features of the plot over the entire temperature range, including the maximum at 5 K. These same parameters also reproduce the magnetization curves at 2 and 5 K (Figure 7), both of which approach 8 μ_B supporting an $S = 4$ ground state. This fit neglects intermolecular interactions, which appears to be a reasonable assumption given the large M···M separations as well as the fact that the D_{Ni} value is in the range of typical values reported for other octahedral Ni complexes.[27]

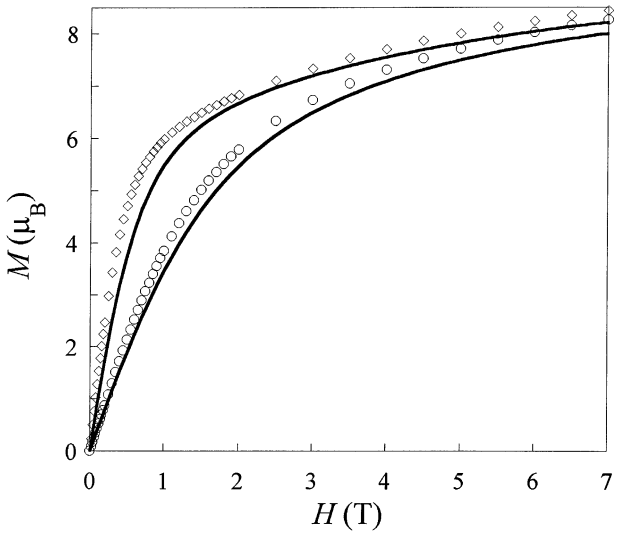

Figure 7. Field dependence of magnetization for compound **1** at $T = 2$ K (◇) and 5 K (○). The solid lines represent the fitting obtained for $g = 2.23$; $J = +4.3$ cm^{-1}; $D_{Ni} = +8.8$ cm^{-1}.

For $[Ni(bpy)_2(OH_2)]\{[Ni(bpy)_2]_2[Fe(CN)_6]_2\}\cdot 12H_2O$ (**2**), (**2**)$\cdot 12H_2O$, the interactions within the square were taken to be the same (defined by the parameter J), and the external Ni^{II}−Fe^{III} interaction was defined by J' (Scheme 2) leading to the Hamiltonian $\hat{H} = -2J[(\hat{S}_{Fe(1)} + \hat{S}_{Fe(2)})\cdot(\hat{S}_{Ni(1)} + \hat{S}_{Ni(2)})] - 2J'[(\hat{S}_{Fe(2)}\cdot\hat{S}_{Ni(3)})] + D[\hat{S}_{Ni(1)z}^2 + \hat{S}_{Ni(2)z}^2 + \hat{S}_{Ni(3)z}^2]$. It is obvious from the best fittings obtained using this model that both interactions, J and J', are of the same sign and very close in magnitude. The fitting of the dc data with J' being less than 80% of the magnitude of J deviates significantly from the experimental curve. The similar values of J and J' do not allow the model to effectively discriminate between the two, and the best fit was obtained for $J = J' = +3.3$ cm^{-1}, $g = 2.25$, and $D_{Ni} = +5.8$ cm^{-1} (Figure 6). As mentioned earlier, g represents a mean value for all atoms and D_{Ni} is the zero-field splitting term for the Ni^{II} ions. This set of parameters satisfactorily reproduces the $\chi_m T$ product throughout the entire temperature range, and also the magnetization curves at 2 and 5 K (Figure 8).

Comments on Previous Reports of Long-Range Magnetic Ordering between Molecules of the Type $\{[Ni(N\text{-}N)_2]_3[Fe(CN)_6]_2\}$. Magnetic data for trigonal bipyramidal clusters similar to that of the new compound $\{[Ni(tmphen)_2]_3[Fe(CN)_6]_2\}\cdot 14H_2O$, (**1**)$\cdot 14H_2O$, have been published in two separate papers, and some puzzling observations were noted. Murray et al. reported that structurally characterized single crystals of $\{[Ni(bpm)_2]_3[Fe(CN)_6]_2\}\cdot 7H_2O$ (bpm = bis(1-pyrazolyl)methane) exhibit long-range magnetic ordering ($T_c = 23$ K) mediated by a hydrogen-bonded network composed of interstitial solvent molecules.[13a] In this same work, they note that associated solids obtained by the rapid combination of reagents do not show reproducible magnetic ordering, leading the authors to deduce that both the crystalline and powder samples contain the same molecular phases, but with different hydrogen-bonding pathways available for magnetic exchange. Similar conclusions were arrived at in a subsequent study in which long-range magnetic ordering was reported for the compound $\{[Ni(bpy)_2]_3[Fe(CN)_6]_2\}\cdot 13H_2O$.[13b] In this

(26) (a) Borrás-Almenar, J. J.; Clemente-Juan, J. M.; Coronado, E.; Tsukerblat, B. S. *Inorg. Chem.* **1999**, *38*, 6081. (b) Borrás-Almenar, J. J.; Clemente-Juan, J. M.; Coronado, E.; Tsukerblat, B. S. *J. Comput. Chem.* **2001**, *22*, 985−991.

(27) (a) Clemente-Juan, J. M.; Coronado, E.; Galán-Mascarós, J. R.; Gómez-García, J. R. *Inorg. Chem.* **1999**, *38*, 55−63. (b) Maslejova, A.; Boca, R.; Dlhan, L.; Papankova, B.; Svoboda, I.; Fuess, H. *Chem. Phys. Lett.* **2001**, *347*, 397−402.

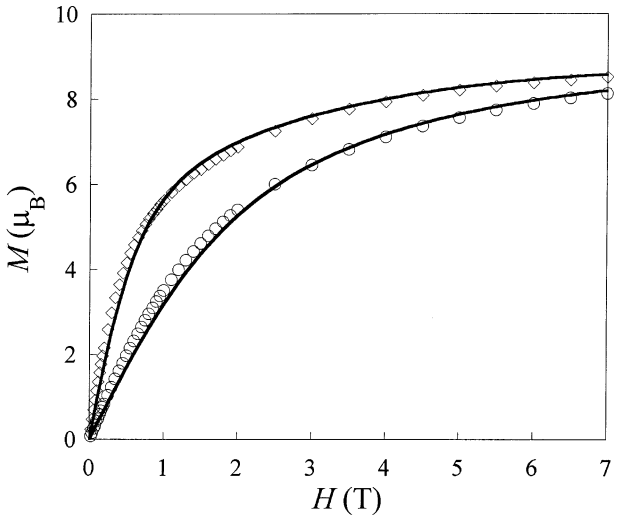

Figure 8. Field dependence of magnetization for compound **2** at $T = 2$ K (◇) and 5 K (○). The solid lines represent the fitting obtained for $g = 2.25$; $J = J' = +3.3$ cm^{-1}; $D_{Ni} = +5.8$ cm^{-1}.

investigation, however, they do not observe magnetic ordering for the crystalline samples, a fact that was attibuted to the desolvation of the crystals.

The aforementioned studies have not provided a direct structural/magneto correlation to support that hydrogen bonding is directly responsible for magnetic ordering.[28] We note that all previous reports of magnetic exchange vis-à-vis hydrogen bonding refer only to the structural role of hydrogen bonding and how it plays an *indirect* role in exchange coupling.[29,30] The claim by Murray et al. that magnetic ordering is propagated via exchange through a hydrogen-bonding network at temperatures as high as 23 K is not consistent with previous reports or previous observations on cyanide-containing magnets. Simply put, how can hydrogen bonding between clusters give rise to magnetic ordering at temperatures as high as the 3-D Prussian blue analogue, $Ni_3[Fe(CN)_6]_2$ ($T_c = 23.6$ K)?[31] Since cyanide-based 2-D networks designed with $[Fe(CN)_6]^{3-}$ units and Ni^{II} building blocks typically exhibit critical temperatures on the order of 9−15 K,[32] and 3-D phases exhibit T_c values >20 K,[4,31] we maintain that long-range magnetic ordering in these discrete clusters remains an open question.

Conclusions

Results from this new study are in accord with earlier reports that slow diffusion reactions between $[Fe(CN)_6]^{3-}$ and $Ni(N\text{-}N)_2L_2$ lead to the formation of discrete molecular species. In this investigation, however, we have also recognized the importance of the role of the solvent and the nature of the co-ligands in determining the resulting geometry of the cluster. Although trigonal bipyamidal clusters with cyanide ligands are well documented, the "extended square" molecular geometry has not been previously observed. It is reasonable to propose that the square motif is the first species to form in solution followed by the addition of a third $\{Ni(N\text{-}N)_2\}^{2+}$ cationic unit to form the neutral extended square structure. When this species remains soluble, the coordinated water molecule is eventually lost and a sixth Fe−CN−Ni interaction forms with closure to the trigonal bipyramidal structure. This is an important observation because it underscores the point that different products are isolated from virtually the same reaction conditions.

The magnetic properties of the two clusters indicate that both molecules exhibit a ground state of $S = 4$ due to intramolecular ferromagnetic coupling. Modeling of the magnetic data leads to similar g, D_{Ni}, and J parameters for the two molecules. There is no evidence of long-range magnetic ordering for well-characterized crystalline samples of both the trigonal bipyramid and extended square clusters. We maintain that it is premature at this stage to conclude that a network of hydrogen bonds can provide a superexchange pathway for magnetic ordering at temperatures as high as 23 K as claimed in the earlier study.[13]

Finally, the subtle synthetic control demonstrated for the present chemistry is being extended to other metal ions. For example, the $[Fe(CN)_6]^{3-}$ and $\{Ni(bpy)_2\}^{2+}$ building blocks are being replaced with $[Mn(CN)_6]^{3-}$ and $\{Co(bpy)_2\}^{2+}$ in an effort to prepare clusters with larger spin ground state values and a higher degree of anisotropy, both of which are important factors in designing high-spin molecules that behave as single molecule magnets.

Acknowledgment. We thank the National Science Foundation for PI and NIRT grants (CHE-9906583 and DMR-0103455) and for equipment grants for the CCD X-ray equipment (CHE-9807975) and the SQUID magnetometer (NSF-9974899). Support from the Welch Foundation and from a Telecommunications and Informatics Task Force (TITF) Grant from Texas A&M University is also gratefully acknowledged.

Note Added after ASAP: The Hamiltonians in the abstract posted ASAP on May 3, 2003, were incorrect. The abstract posted ASAP on May 16, 2003, contains the correct Hamiltonians.

Supporting Information Available: Details of the magnetic measurements, TGA data, and ac susceptibility measurements for molecules **1** and **2** and the magnetic properties of the insoluble solids.[20,21] Crystallographic data in CIF format. This material is available free of charge via the Internet at http://pubs.acs.org.

IC0205031

(28) Desplanches, C.; Ruiz, E.; Alvarez, S. *Chem. Commun.* **2002**, 2615−2615.
(29) (a) Bertrand, J. A.; Helm, F. T. *J. Am. Chem. Soc.* **1973**, *95*, 8184−8185. (b) Pei, Y.; Kahn, O.; Nakatani, K.; Codjovi, E.; Mathoniere, C.; Sletten, J. *J. Am. Chem. Soc.* **1991**, *113*, 6558−6564. (c) Xie, Y.; Bu, W.; Xu, X.; Jiang, H.; Liu, Q.; Xue, Y.; Fan, Y. *Inorg. Chem. Commun.* **2001**, *4*, 558−560.
(30) Moron, M. C.; Palacio, F.; Pons, J.; Casabo, J.; Solans, X.; Merabet, K. E.; Huang, D.; Teo, B. K.; Carlin, R. L. *Inorg. Chem.* **1994**, *33*, 746−753.
(31) Juszczyk, S.; Johansson, C.; Hanson, M.; Ratuszna, A.; Malecki, G. *J. Phys.: Condens. Matter* **1994**, *6*, 5697−5706.
(32) (a) Kou, H. Z.; Gao, S.; Bu, W. M.; Liao, D. Z.; Ma, B. Q.; Jiang, Z. H.; Yan, S. P.; Fan, Y. G.; Wang, G. L. *J. Chem. Soc., Dalton Trans.* **1999**, 2477−2480. (b) Kou, H.-Z.; Gao, S.; Ma, B.-Q.; Liao, D.-Z. *Chem. Commun.* **2000**, 1309−1310.